Berit Mueller, Laura Treccani and Kurosch Rezwan

Antibacterial active open-porous hydroxyapatite/lysozyme scaffolds suitable as bone graft and depot for localised drug delivery

Antibacterial active open-porous hydroxyapatite/lysozyme scaffolds suitable as bone graft and depot for localised drug delivery

Berit Mueller, Laura Treccani and Kurosch Rezwan

Abstract

An engineered synthetic scaffold for bone regeneration should provide temporary structural support and a medium for controlled and localised release of bioavailable medical drugs. In this work, a method is proposed to incorporate biologically active agents without impairing agent activity into open-porous resorbable hydroxyapatite scaffolds. Scaffolds are obtained by a one-pot freeze gelation process and loaded with different amounts of lysozyme, a model macromolecular drug with antibacterial activity. The antibacterial activity is tested by submerging hydroxyapatite scaffolds with 0.5 to 2.5 wt.% lysozyme into two different bacteria stock solutions. A complete dieback of *M. luteus* bacteria when in contact with the scaffolds is observed. Higher lysozyme amount in the scaffold leads to faster dieback. In contact with scaffolds containing 2.5 wt.% lysozyme after 30 min, no viable bacteria can be observed. An amount of 0.5 wt.% lysozyme in the scaffolds is sufficient to kill all bacteria after a contact time of 24 h. For *L. innocua*, a bacteriostatic effect is observed. The scaffolds have *spongiosa*-like stability and are suitable bone implant substitutes. As agents are released from the scaffolds by degrees over a time period of at least 9 days, they are particularly attractive as depot for localised drug delivery of bioactive macromolecular drugs.

Keywords

Antibacterial activity, bioresorption, drug delivery system, hydroxyapatite, lysozyme

Introduction

Engineered scaffolds are nowadays widely used for restoration of bone tissues damaged by tumours, musculoskeletal disorders (e.g. osteoporosis and osteoarthritis) or complicated fractures.[1] Ideally, synthetic scaffolds have to restore, maintain or improve tissue function. They must provide a temporary stabilisation until new bone forms in the defect sites,[2] and simultaneously stimulate cell growth and osteoregeneration. Further, scaffolds must contain therapeutically active agents that can be delivered and trigger the healing process, accelerate bone tissue formation and suppress inflammatory reactions or bacterial infections.[3–5]

There are different possible routes of administration for most drugs, which can be broadly divided into two categories: systemic and local. Conventional methods for systemic drug delivery are oral administration and injection. Oral administration is most convenient for the patient but can only be applied for small molecules (e.g. antibiotics and steroid hormones). Macromolecular drugs such as proteins, protein hormones and enzymes must be administered by injection[6–8] which, in most cases, cannot be conducted by the patient himself. Both injection and oral administration are routinely used, but they cannot ensure a sufficient concentration of active drugs at the defect site due to the poor penetration into the targeted tissue and can even cause systemic toxicity.[9,10]

Local drug delivery is considered a promising alternative to oral administration and injection. The side effects and risk of overdose are limited, and it is more effective as a higher drug concentration can reach

University of Bremen, Germany

Corresponding author:

Laura Treccani, Petroceramics SPA, c/o Kilometro Rosso Science & Technology Park, Viale Europa 2, 24040, Stezzano (BG), Italy.

Email: treccanilaura@gmail.com

the targeted site. In addition, it permits controlled delivery at a specific rate and for a specific period of time at the desired location.

Drug delivery rate and profile of a particular drug are key issues and they are mainly determined by the matrix used as carrier and by the loading method applied. Several methods have been developed for active drug incorporation, but only few can be used for fabricating scaffolds with therapeutic drug-delivery capability. Moreover, several approaches use carrier materials or processes not adequate for large scale production or clinical applications.[11]

For instance, the most common approaches for drug immobilisation in synthetic scaffolds are adsorption, covalent attachment and self-assembly.[12,13] The drugs are immobilised on the scaffold surface and their amount is limited by the pore size and surface area of the scaffold, and their activity can be limited by the immobilisation itself.

Biomolecular drugs are susceptible to damage by heat, mechanical agitation, radiation, pH shift and certain chemicals as for example organic solvents. All these factors, if deployed in to high degrees during processing, can lead to denaturation by loss of molecule structure and ultimately to loss of function.[14–17] As virtually all conventional ceramic moulding processes involve one or more of the enumerated factors,[18] the processing for the fabrication of protein-containing scaffolds must be customised so as to prevent drug damage.

As recently reported in an own previous publication, it is possible to produce biocompatible, resorbable, open-porous hydroxyapatite/protein scaffolds by the one-pot freeze gelation method (OPFG).[19] It permits the direct incorporation of large and controllable amounts of macromolecules without additional processing steps. We have shown that the OPFG method can be effectively used for the incorporation of both acidic and alkaline model proteins.[19–22] This suggests that such method is versatile and can be employed to incorporate also other biological compounds like temperature-sensitive biomolecules and growth factors.

The biocompatibility and resorbability of such scaffolds has been already shown by in vivo tests.[19] Hydroxyapatite (HAp) scaffolds with 5 wt.% LSZ content implanted in domestic pigs did not cause inflammation and showed material resorption of over 50% and new bone formation of 21% after 8 weeks.

In this article, we intend to show the feasibility of the method to create scaffolds capable of long-term release and simultaneously able to protect sensible incorporated biomolecules from irreversible inactivation. To demonstrate this, we used lysozyme (LSZ) as a model macromolecular drug. LSZ is an antibacterial enzyme present in body secretions like saliva, blood and tear fluid able to destroy gram-positive bacteria and widely used as preservative in foods, medical and cosmetic products.[23]

LSZ was incorporated in HAp scaffolds. HAp is a widely applied material for the fabrication of biocompatible and resorbable synthetic scaffolds.[24–26] HAp scaffolds containing 0.5, 1.0, 1.5 and 2.5 wt.% LSZ and without LSZ were fabricated by the OPFG process. The scaffolds were characterised in terms of porosity, mechanical strength, protein release and antibacterial effect to demonstrate their suitability as bone replacement material and drug delivery system.

Materials and methods

Materials

Hydroxyapatite powder (HAp, particle size of 100 nm, specific surface area of 65 g/m^2,[22] Prod. No. 04238), lysozyme (LSZ, lyophilised powder from chicken egg white, purity > 90%, Prod. No. L6876), agar (Prod. No. A7002) and phosphate-buffered saline (PBS, Prod. No. P4417) were obtained from Sigma Aldrich (Germany). Anhydrous citric acid (Prod. No., 27488, Fluka, Germany), concentrated ammonia solution (Prod. No. 105432, Merck, Germany), ammonia stabilised silica sol (solid content of 30 wt.% and particle size of 8 nm, Bindzil 220/30 NH_3, EKA, Germany), o-cresolphthaleincomplexone assay (Fluitest® Ca CPC, Analyticon, Germany) and McFarland turbidity standard (Prod. No. R20421, Remel, Germany) were purchased from different suppliers as specified.

For the bacterial tests, the gram-positive strains *Micrococcus luteus* (*M. luteus*, Cat. No. 20030, DSMZ) and *Listeria innocua* (*L. Innocua*, *Cat. No.* 20649) and the gram-negative strains *Escherichia coli* (1077, DSMZ) and *Pseudomonas fluorescens* (*P. fluorescens*, Cat. No. 50090 DSMZ) were obtained from the Deutsche Sammlung von Mikroorganismen und Zellkulturen GmbH, Germany. The nutrients brain heart infusion (Prod. No. 53286, Fluka) and lysogeny broth (Prod. No. L3022, Sigma Aldrich) were obtained for bacteria cultivation. Double deionised water (ddH_2O) with an electrical resistance of 18 MΩ (Synergy®, Millipore, Germany) was used for all experiments.

Scaffold fabrication and characterisation

The scaffolds were fabricated by a OPFG process schematically described in Figure 1 and according to our previous study.[19] Briefly, suspensions were obtained by mixing ddH_2O with silica sol (1 wt%) and citric acid (0.5 mg/m^2) and adding HAp powder gradually under constant stirring. Citric acid was used as dispersant and its amount was normalised on the HAp powder specific

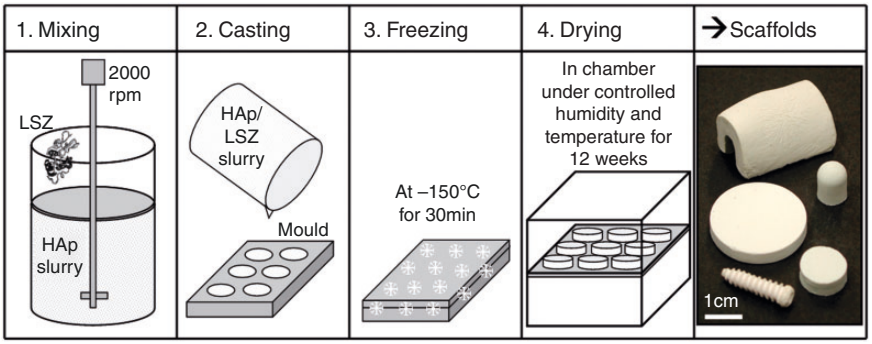

Figure 1. Schematic of the one-pot freeze gelation (OPFG) process. The direct mixing of the proteins into the slurry enables the fabrication of HAp/LSZ scaffolds in a one-step process. After casting and freezing, the water in the suspension forms open-porous channels within the scaffold. By addition of freeze-sensitive silica sol, a sufficient mechanical strength of the scaffold green bodies is obtained and no further sintering steps are required. The process allows the near-net-shape fabrication of customisable parts as representatively shown.

surface area. The specific surface area of HAp corresponded to 65 m^2/g and it was quantified by nitrogen adsorption (Gemini, Micromeritics) as previously reported.[19] The suspension was stirred with a high speed stirrer (Dispermat LC-2, VMA-Getzmann GmbH) at velocities up to 2000 rpm. As HAp suspensions are only stable in alkaline milieu, the pH was adjusted to 8 by adding drop wise concentrated ammonia solution. After homogenisation, LSZ powder was added to the slurry in concentrations of 0.5, 1.0, 1.5 and 2.5 wt.% and stirred for 5 min at 2000 rpm. The amount of LSZ is relative to the suspension's solid content.

Afterwards, the slurry was poured into moulds made of plasticised polyvinyl chloride and frozen at −150°C for 30 min (Freezer MDF-1156ATN, Sanyo E&E Europe BV, UK). By freezing, ice channels are generated leading to interconnected porosity in the scaffolds after drying. After demoulding, the scaffolds were dried at room temperature and defined relative humidity (RH). First, the samples were slowly dried at 97% RH for 7 days in order to avoid crack formation. Afterwards, they were stored at 30% RH for 12 weeks. Five different scaffold types were produced for the experiments: scaffolds with 0.5, 1.0, 1.5 and 2.5 wt.% LSZ and scaffolds without LSZ (0 wt.%) used as reference.

The mechanical strength of the scaffolds was determined by a biaxial flexure strength test, the ball on three balls test according to Borger et al.[27] For this test, disc-shaped specimens of 28 mm in diameter and 4.5 mm in height were placed on three balls arranged in a circle and punched by one ball from above positioned in the middle of the disc. The experiments were conducted with a compression-tension testing machine (Zwick Z005, Zwick, Germany). Eight specimens for every scaffold type were used. The Poisson's ratio for porous HAp ceramics was obtained from Ren et al.[28] and corresponds to 0.25. The total porosity of the scaffolds was calculated by taking into account material density, dimensions and specimen weight. The interconnected porosity was measured by mercury intrusion porosimetry (Pascal 140/440, Porotec, Germany). Images of the scaffolds' texture and microstructures were obtained by scanning electron microscopy (SEM; Cambridge Scan, Cambridge Instrument Company, UK). All specimens were sputtered with a thin gold layer (sputter coater 108 Auto, Cressington, USA).

LSZ and Ca^{2+} release was measured using cylindrical specimens of 14 mm in diameter and 5.5 mm in heights. The specimen were immersed in 8 ml PBS and 0.2 ml of supernatant was removed after 10 min, 30 min, 1 h, 2 h, 4 h, 8 h, 12 h, 24 h and 32 h without replacement so as to avoid deviation from bacteria testing conditions. The measurements were done in triplicates. The amount of released LSZ was determined using a Bradford protein assay (Prod. No. P500-0006, Bio-Rad).[29] The absorbance was measured at a wavelength of 595 nm (Xion 500, Dr. Lange GmbH). LSZ solutions with different concentrations were used as standard curves to extrapolate LSZ concentration.

The amount of released Ca^{2+} in the supernatant was quantified using o-cresolphthaleincomplexone as described elsewhere.[20] Briefly, 2 ml of the assay reagent was added to 50 µl of supernatant and incubated for 15 min at room temperature. The absorbance was measured at 570 nm. The calcium concentration was calculated using standard curves (serial dilution of $CaCl_2$, 0–200 µg/ml). The release tests followed the procedure of the optical density bacterial tests (see next section).

Bacterial tests

The antibacterial properties and LSZ activity of the specimens were determined with three different

assays: optical density measurements, total viability counts and zone of inhibition tests (Kirby–Bauer tests[30]). The optical density measurements and total viability counts were done with two gram-positive (*M. luteus* and *L. innocua)* and two gram-negative (*E. coli* and *P. fluorescens*) bacteria strains. For the zone of inhibition tests, only the *M. luteus* strain was used. Prior to the bacterial tests, all scaffolds were gamma-sterilised at a dosage of 25 kGy. These conditions were selected as used for commercial-scale sterilisation of medical supplies.[31]

Agar plates were obtained by filling sterilised Petri dishes with autoclaved, 60°C tempered agar medium enriched with 5 wt.% of nutrient. Brain heart infusion was used as nutrient for *M. luteus* and *L. innocua*, whereas lysogeny broth was used for *E. coli* and *P. fluorescens*.

Bacteria were cultivated on agar plates and afterwards suspended in nutrient broth at a temperature of 20°C for 18 h. Bacteria were recollected by centrifugation at 2500 rpm for 10 min, dissolved in sterilised PBS and diluted to an optical density of 0.12, which corresponds to a bacteria concentration of 3×10^8 CFU/ml according to the McFarland turbidity standard. Cylindrical specimens (14 mm in diameter and 5.5 mm in height) were immersed in 8 ml of the prepared bacteria stock solutions of the two different bacteria strains. For each scaffold type (with 0, 0.5, 1.0, 1.5 and 2.5 wt.% LSZ), five specimens were used and separately analysed. The optical density was measured by a plate reader (Plate CHAMELEON V, Hidex) using 0.2 ml of bacteria solution collected after 10 min, 30 min, 1 h, 2 h, 4 h, 8 h, 12 h, 24 h and 32 h.

In addition, LSZ control measurements were conducted by adding different amounts of LSZ to 8 ml bacteria stock solution resulting in two different LSZ concentrations (0.5 and 0.05 mg/ml). Throughout the experiments, the testing tubes (Cat.-No. 525-0304, VWR) with the specimens and the bacteria solutions were kept at a constant temperature of 20°C and shaken to avoid bacteria sedimentation.

For total viability counts, bacteria supernatant was removed after 8 and 24 h and diluted with PBS. As the bacteria concentration widely differed throughout the experiments for each measurement point, several dilutions between 1 and 100,000 were required to obtain reliable results. Optical density measurement results were used as reference points. The diluted bacteria suspension was uniformly spread with a Drigalski spatula on the agar plates and kept at 20°C for 3 days. Afterwards, the number of CFU was counted only considering plates with less than 300 colonies.

For the zone of inhibition tests, three specimens of each sample type were imbedded in BHI-agar cooled down to 40°C. This was necessary as the scaffolds were too heavy to be supported by the agar layer. Afterwards, 0.33 ml of bacteria solution was dispersed on the prepared BHI-agar plates. After 3 days of cultivation time at 20°C, samples were photographed to measure the size of the inhibition zone. All processing steps were done with sterilised media and under a clean bench to avoid any contamination.

Results

Scaffold characterisation

A schematic of the fabrication process and green bodies with different sizes and shapes are representatively shown in Figure 1. The OPFG method permit the creation of scaffolds with specific shapes and different geometries by using different moulds, thus enabling customisable scaffolds that can perfectly match bone defects. By freezing of the suspension, the HAp particles are moved apart from the ice crystals. After ice evaporation, porous microstructures are formed and are a negative replica of the ice crystals. The use of silica sol can be used to enhance scaffold stability and confer sufficient mechanical strength to green bodies. In fact, it has freeze sensitive properties and induces an irreversible gelling of the scaffold during freezing.[32]

Biaxial flexure strength vs. total porosity is plotted in Figure 2(a). SEM images of polished sections of the scaffolds are given in Figure 2(b). The biaxial flexure strength was varying between 1.7 ± 0.1 MPa (with 0.5 wt.% LSZ) and 5 ± 0.6 MPa (2.5 wt.% LSZ). Likewise, the total porosity was varying between $63 \pm 0.6\%$ (0.5 wt.% LSZ) and $55.4 \pm 1.3\%$ (2.5 wt.% LSZ). Scaffolds without LSZ had a strength of 3.6 ± 0.7 MPa and a porosity of $56.5 \pm 0.9\%$. All scaffolds had an average nano-pore size of around 50 nm measured by mercury intrusion porosimetry. SEM images (Figure 2(b)) revealed larger micropores with lamellar morphology up to 100 μm in length in scaffolds with 0.5 and 1.0 wt.% LSZ, which moreover showed an alignment. In contrast in scaffolds with 0.0, 1.5 and 2.5 wt.% pores had a size up to 5 μm and cellular morphology. According to mercury intrusion porosimetry, measurements over 90% of the total pore volume was interconnected.

The water evaporation during the drying period led to a shrinkage of $25 \pm 1\%$ for scaffolds with 0.0, 1.5 and 2.5 wt.% LSZ. The scaffolds with larger pores (1.0 and 0.5 wt.% LSZ) had a shrinkage of 21 and 15%, respectively.

The behaviour of the dried scaffold in contact with liquids, the release of calcium ions and LSZ molecules loaded in the scaffold, was considered up to 32 h. When immersed in liquid, the dried scaffolds remained intact. As shown in Figure 3, two main LSZ release pattern

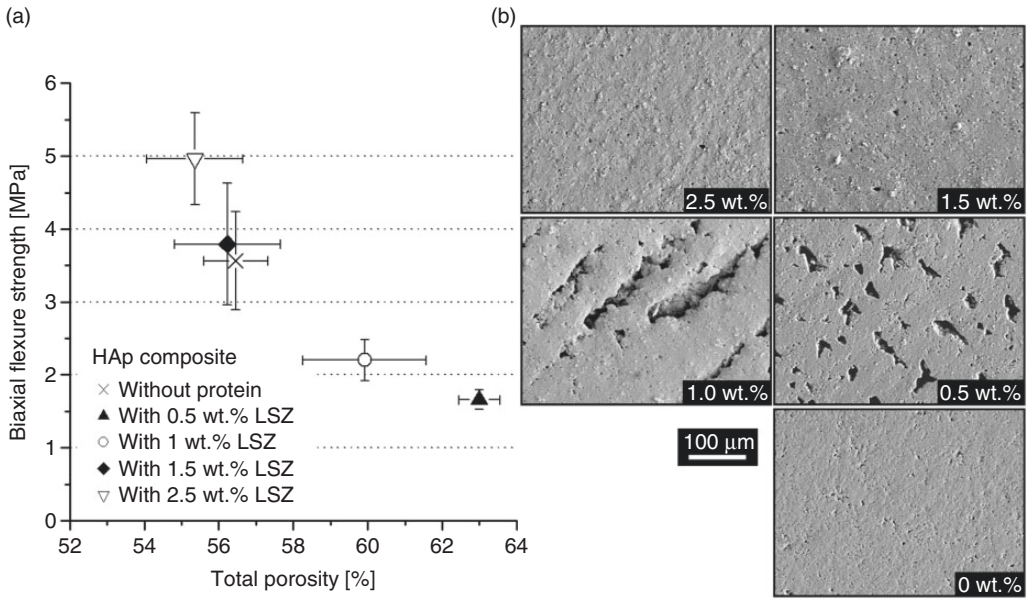

Figure 2. (a) Incorporation of LSZ into HAp scaffolds influences their mechanical strength. Scaffolds with 2.5 wt.% LSZ showed an increased biaxial flexure strength of 5.0 ± 0.6 MPa as compared to protein-free scaffolds with 3.6 ± 0.7 MPa. For scaffolds with 0.5 and 1.0 wt.% of LSZ, a reduced flexure strength compared to protein-free scaffolds was found. The mechanical strength of the scaffolds is strongly influenced by their different total porosity. (b) SEM images of the scaffolds with 0.5 and 2.5 wt.% are given to illustrate the different textures.

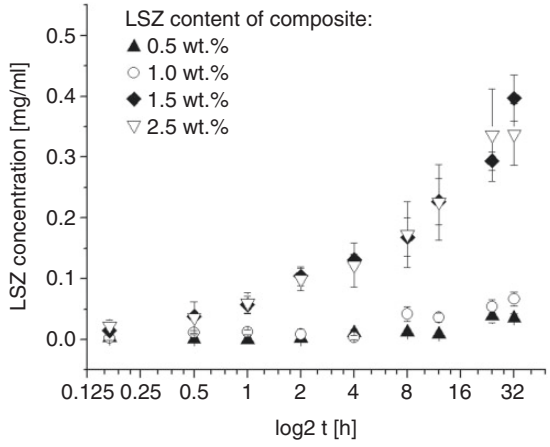

Figure 3. LSZ release of HAp scaffolds with 0.5, 1, 1.5 and 2.5 wt.% LSZ in PBS solution over a period of 32 h determined by VIS spectroscopy.

can be identified as a function of the incorporated LSZ. The amount of LSZ is expressed in mg/ml to correlate with the amount of LSZ used for bacterial tests. The highest LSZ release up to 0.40 mg/ml was observed after 32 h for scaffolds with 1.5 wt.% and 2.5 wt.% LSZ. The concentration of LSZ released corresponds to ~15% and ~8% of the initial quantity of protein introduced in 1.5 wt.% LSZ and 2.5 wt.% LSZ scaffolds, respectively. A lower LSZ release (~0.05 mg/ml after 32 h) was observed for scaffolds with 0.5 and 1.0 wt.% LSZ corresponding to 3.9 and 3.8% of the initial LSZ content, respectively.

Figure 4 shows the Ca^{2+} release in demineralised water (a) and in PBS (b). Ca^{2+} release amounts lower than 10^{-4} M were found in PBS. After 24 h, no Ca^{2+} could be measured as Ca^{2+} concentration was below the assay detection limit (corresponding to 0.05 mmol/l). For scaffolds with 0.5 wt.% LSZ, all values were under the detection limit. For comparison, Ca^{2+} release was also observed in demineralised water leading to 10 times higher values (a).

Bacterial tests

The antibacterial efficacy of the HAp/LSZ scaffolds and released LSZ against both gram-positive bacteria *M. luteus* and *L. innocua* were evaluated in vitro during a period of 32 h using different assays.

The activity of LSZ released from HAp/LSZ scaffolds was monitored with *M. luteus* by means of a zone of inhibition test, also called a Kirby–Bauer test. This test is used clinically to determine the ability of antimicrobial agents to inhibit microbial growth. If the bacterial strain is susceptible to the antimicrobial agent, a clear zone (the zone of inhibition) appears on the agar plate around the specimen. The formation of inhibition on the agar plates was observed around all HAp/LSZ scaffolds but not around the scaffolds

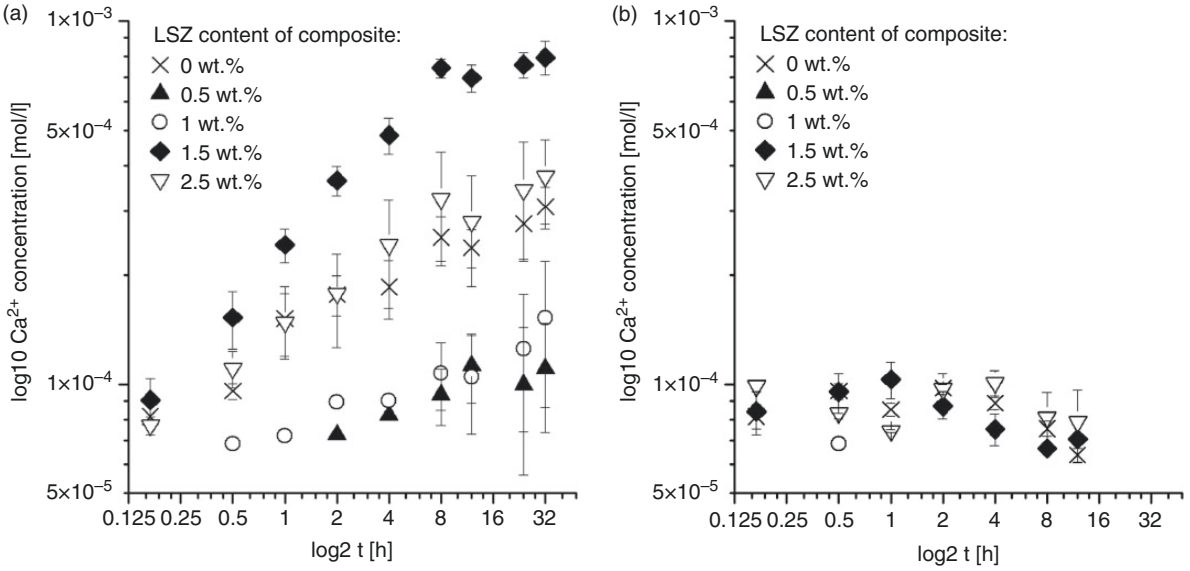

Figure 4. Ca^{2+} release of HAp scaffolds with 0, 0.5, 1.0, 1.5 and 2.5 wt.% LSZ over a 32-h-time-period as determined by VIS spectroscopy (a) in demineralised water and (b) in PBS. In demineralised water, Ca^{2+} release reaches a plateau value at 8 h for all scaffold types. Under experimental conditions in PBS, the Ca^{2+} release is on average 10 times lower.

without protein. Some representative images taken after 3 days cultivation (Figure 5(a) to (e)) show that the extension of the inhibition zone is proportional to the amount of LSZ contained in the scaffold (Figure 5(f)). The largest inhibition was observed for scaffolds containing 2.5 wt.% LSZ.

The antibacterial activity of LSZ released from the HAp/LSZ scaffolds was measured with *M. luteus* and *L. innocua* by means of turbidimetric and total viability tests (Figure 6). The bacteria stock solutions (initial bacteria concentration of 3×10^8 CFU/ml) and LSZ-free scaffolds were used as a reference.

The bacteria concentration in the stock solution was screened by total viability counts after 8 and 24 h. For *L. innocua*, both at 8 and 24 h, the bacteria concentration was close to the initial concentration of the stock solution (3×10^8 CFU/ml). The number of *M. luteus* in stock solution was also constant over the observed time period. However, counts yielded only 0.8×10^8 CFU/ml after 8 and 24 h, presumably related to the slower growth rate of *M. luteus* in comparison to *L. innocua*. Therefore, fewer *M. luteus* colonies became visible.

A dieback of *M. luteus* and a growth inhibition for *L. innocua* in contact with HAp/LSZ scaffolds were observed during a time period of 32 h. Scaffolds with 2.5 wt.% LSZ showed the highest antibacterial activity and an optical density corresponding to 0 CFU/ml was measured after 30 min. In contrast, scaffolds with 0.5 wt.% LSZ showed a slower decline in bacteria concentration. After 32 h, the OD corresponded to 0.19×10^8 CFU/ml denoting that only 0.006% of added bacteria were still alive (Figure 6(a)). The total viability count test confirmed these results (Figure 6(b)). After 8 h, viable *M. luteus* bacteria could only be detected for scaffolds with 0.5 wt.% LSZ. After 24 h, no viable bacteria were observed for any LSZ containing scaffolds. The scaffolds without LSZ showed bacteria numbers after 8 and 24 h of 1.4 and 0.6×10^8 CFU/ml, respectively, and an increased optical density as compared to the stock solution was observed beginning at 2 h.

For *L. innocua*, the optical density remained constant for all samples up to 4 h. After 8 h, a slight increase in optical density could be observed for all samples (Figure 6(c)). The total viability counts revealed an almost equal bacteria number for all samples. Measurements after 8 and 24 h yielded similar results for all scaffold types (Figure 6(d)).

E. coli and *P. fluorescens* showed constant bacteria concentration up to 4 h. Subsequently, strong bacteria proliferation both in contact with LSZ-free and LSZ-containing scaffolds was observed (data not shown).

The effect of LSZ on the bacteria strains was observed in a control experiment using freshly prepared LSZ solutions. LSZ was added to each bacteria stock solution at concentrations of 0.05 and 0.5 mg/ml. The concentrations were chosen to resemble the two main LSZ release pattern (Figure 7). Both for 0.05 and 0.5 mg/ml LSZ concentration, all *M. luteus* bacteria were killed after 24 h. For *L. innocua*, the cell number decreased up to 70% for 0.05 mg/ml LSZ and up to 92% for 0.5 mg/ml LSZ (Figure 7).

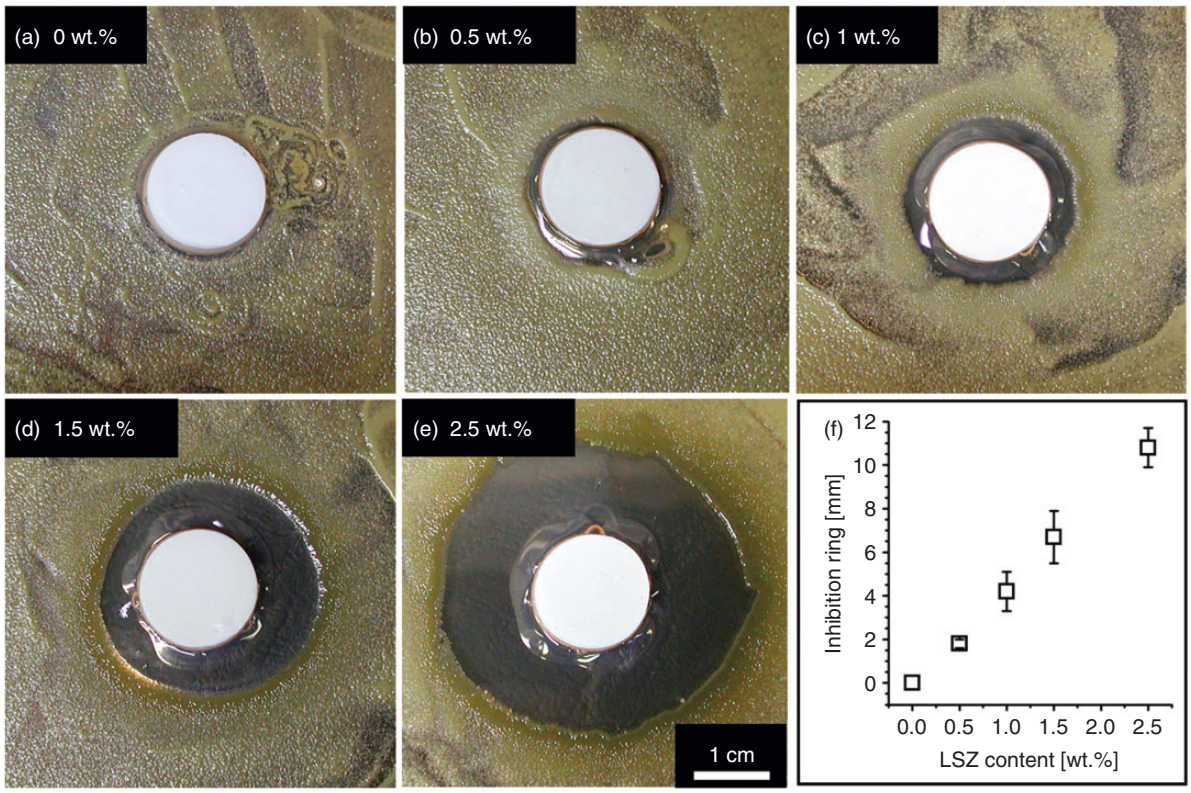

Figure 5. Qualitative analysis of the antibacterial effect of HAp/LSZ scaffolds on gram-positive bacteria. Scaffolds were embedded in agar plates and cultivated for 3 days with 10^8 *M. luteus* bacteria cells each. For LSZ containing scaffolds, an inhibition zone around the specimens is developed (b–e). The size of the inhibition zone increases with increasing LSZ content. The average inhibition zone size is given in (f).

Discussion

In this study, we showed that the OPFG process permits the fabrication of porous scaffolds, which can incorporate sensitive biomolecules directly in the slurry and they remain active over a long-time period. The scaffolds feature an interconnected porosity and the porosity and strength of all fabricated scaffold types are in the range of human *Spongiosa*.[33–35] Moreover, this method enables the fabrication of scaffolds with customisable geometries and shapes. All these features make the scaffold suitable for usage in tissue engineering.

The freeze-sensitive silica sol, which can irreversibly gel, induces the stabilisation of the interconnected porosity formed by the ice channels and imparts sufficient strength to the overall green body structure. This makes any further heat treatment unnecessary and the green scaffolds can be easily handled, e.g. facilitating their use in clinical settings.

The biaxial flexure strength of the scaffolds is only indirectly affected by the presence of protein, although it seems to increase with increasing LSZ content (with the exemption of protein-free scaffolds). In fact, when biaxial flexure strength is plotted against the scaffolds' total porosity (Figure 2(a)), it becomes apparent that the strength depends on porosity only, and a direct influence of LSZ on scaffold strength cannot be observed. In addition, the lamellar, aligned micropores in scaffolds with 0.5 and 1.0 wt.% LSZ led to less stability as compared to the other scaffold types. With increasing LSZ content, the porosity is decreasing leading to higher mechanical stability. The porosity of protein-free scaffolds is close to the porosity of scaffolds with 1.5 wt.% LSZ. Hence, both scaffold types have comparable biaxial flexure strength. The poor or no influence of LSZ on the scaffolds' strength seems to be directly related to LSZ inability for networking. We have shown in a previous study that other proteins with networking capability, like BSA and fibrinogen, have a direct influence on the mechanical properties of scaffolds obtained by the OFPG-process.[19,20]

The porosity and structure of freeze casted scaffolds is dependent on many factors, among others particle size, solid concentration in the slurry, sample shape and the influence of additives.[36,37] The use of nano-HAp suppresses the formation of aligned pores

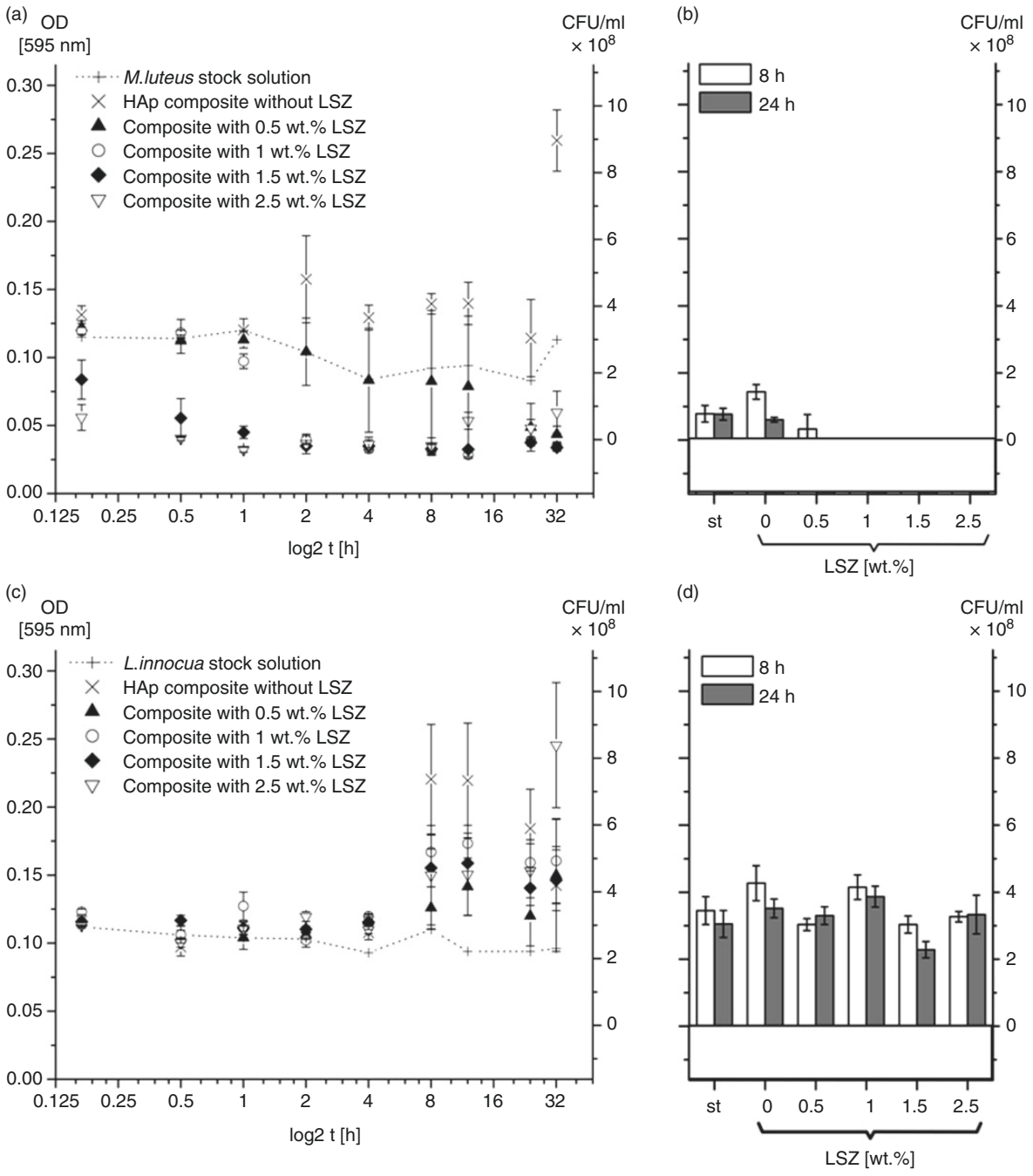

Figure 6. Proliferation of gram-positive bacteria in the presence of HAp/LSZ scaffolds determined by optical density measurements over a period of 32 h (a,c) and by total viability counts after 8 and 24 h (b,d). The experiments were carried out for the bacteria stock solutions (st) and for scaffolds with 0, 0.5, 1, 1.5 and 2.5 wt.% LSZ. The dotted lines in (a) and (c) represent the viability of the bacteria of stock solutions. As LSZ damages the cell walls of gram-positive bacteria, *M. luteus* cells (a,b) are destroyed and the proliferation of *L. innocua* cells (c, d) is prevented.

and promotes the formation of numerous small pores as more nucleation sites for ice crystal growth are generated due to greater surface area.[38] Indeed, the formation of aligned pores is suppressed in scaffolds with 0, 1.5 and 2.5 wt.% LSZ. However, when LSZ is added in concentrations of 0.5 and 1.0 wt.% aligned pores are formed with pore diameters up to 100 µm. The influence of protein on the structure of freeze casted scaffolds has been investigated in a few studies where gelatine (hydrolysed protein) was used as additive.[36,39,40] These works also reveal different pore morphologies and sizes dependent on gelatine concentration.

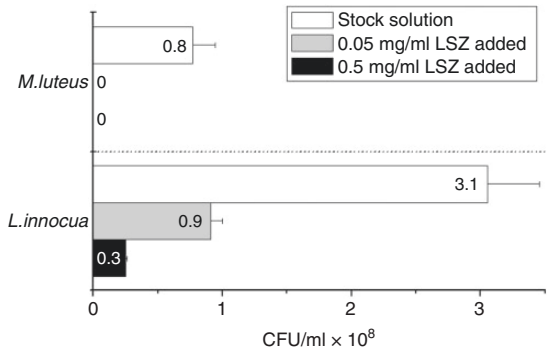

Figure 7. As a control, the effect of pure LSZ on the bacteria proliferation after 24 h was detected. LSZ was added to the stock solution of every bacteria strain at two different concentrations (0.05 and 0.5 mg/ml) according to the scaffolds' LSZ release. The numbers given on the bars represent total viability counts after 24 h. LSZ inhibits the proliferation of both gram-positive bacteria strains. A LSZ concentration of 0.05 mg/ml suffices to kill all *M. luteus* cells have died after 24 h. *L. innocua* shows a slightly higher resistance to LSZ. A LSZ addition of 0.5 mg/ml leads to a decrease in cell number of 92% after 24 h relative to the *L. innocua* stock solution.

For example, Zhang et al., which however used a different solid content and HAp powder with different particle size, observed up to 5 times larger-sized pores for scaffolds with 2 wt.% as compared to scaffolds with 6 wt.% gelatine.[39]

The results demonstrate that the antibacterial effect of LSZ is not impaired by the processing, even though LSZ molecules are subjected to mixing at high speed up to 2000 rpm, freezing at −150°C and drying for 12 weeks (Figure 1). This suggests that the process is suitable for the preservation of drugs and facilitates the scaffolds off-the-shelf application. Figure 5 shows by means of a zone-of-inhibition experimental set-up how HAp/LSZ scaffolds clearly inhibit the growth of gram-positive *M. luteus* bacteria. The diameter of the inhibition ring that developed around the LSZ-containing scaffolds is linearly dependent on the amount of LSZ in the scaffold. The antibacterial property depends only on active LSZ molecules released from the scaffolds and is not influenced by other agents used for processing. For instance, the citric acid used for slurry stabilisation is one of the most common food additives both for flavouring and, due to its antibacterial properties, also as preservative.[41,42] However, the applied concentration used in this study is too low to have a significant antibacterial effect.[43] An impact of gamma-sterilisation on LSZ activity could not be observed either. This goes along with other findings showing that gamma-sterilisation up to a dosage of 25 kGy does not or only minimally impair enzymatic activity.[44,45] However, the extent of damage by gamma-sterilisation may vary dependent on the specific biomolecule, so that the applied dosage of gamma sterilisation must be ascertained for the deployed drug individually.[46]

A quantitative study on the antibacterial effect of LSZ on two gram-positive strains was carried out by turbidimetric measurements and total viability counts. The results of both methods are in good correlation with each other. The HAp/LSZ scaffolds had an antibacterial effect on both gram-positive bacteria strains. In the case of *M. luteus*, all bacteria were destroyed. In the case of *L. innocua*, an increase in bacteria number could be prevented denoting a bacteriostatic effect (Figure 6). For *M. luteus*, a LSZ amount of 0.5 wt.% in the scaffolds, corresponding to a maximum concentration of 0.04 mg/ml in the experimental setting, was sufficient to destroy all bacteria after 24 h. Higher amounts of LSZ in the scaffold led to even faster dieback.

The effect of the HAp/LSZ scaffolds on gram-negative bacteria was also investigated with the bacteria strains *E. coli* and *P. fluorescens*. A bacteriostatic effect was observed up to 4 h, and after 4 h, bacteria proliferation increased. This finding is not surprising as gram-negative bacteria are generally resistant to LSZ as they have thicker and more stable cell walls than gram-positive bacteria.[47] However, experiments showed that LSZ can destroy gram-negative bacteria under certain circumstances, for example, if modified by fatty-acid-attachment[48] or if combined with lactoferrin, another antibacterial protein.[49] In this way, LSZ could be deployed against a wider range of bacteria strains.

In several studies, a comparably higher biofilm formation was observed on HAp surfaces than on other ceramic surfaces as zirconia, metal surfaces as Ti or Co/Cr, and even natural surfaces as bovine bone.[50–52] Thus, the appliance of antibacterial agents in connection with HAp-based bone replacement materials is highly important. The high affinity of HAp scaffolds to biofilm formation could also explain why a bacteria dieback could not be reached for *L. innocua* when in contact with HAp/LSZ scaffolds, though reference experiments showed a clear antibacterial effect of LSZ on *L. innocua* (Figure 7).

Though LSZ has a solubility of up to 10 mg/ml, the release rate was low indicating that the HAp scaffolds protected the protein from uncontrolled release. After 32 h, a maximum concentration of 0.4 mg/ml was dissolved for scaffolds with 1.5 and 2.5 wt.% LSZ content. This corresponds to a release rate of 0.1 mg/h. For scaffolds with lower LSZ content, 0.5 and 1.0 wt.%, the release rate was only 0.02 mg/h. The highest percentage of LSZ released in the experimental setting after 32 h corresponded to 15 wt.% denoting that a protein

content of 85 wt.% and higher remained in the scaffolds. The slope of the release curves did not decrease up to 32 h, indicating ongoing release also for longer time periods (Figure 3). The release is regulated by initial protein content and porosity. The open porosity of the scaffolds combined with mostly nanometre-scale pore diameters secures slow drug release. The antibacterial tests showed that the low release rates were sufficient to kill bacteria.

In a previous study, HAp/LSZ scaffolds with 5 wt.% LSZ content were tested in vivo in domestic pigs and did not only produce no inflammation but showed material resorption of over 50% and new bone formation of 21% after 8 weeks.[19] In another previous study, it could be shown by adsorption experiments with model proteins that HAp powder can bind both alkaline and acidic proteins in almost equally high amounts.[22] This renders the method suitable for the sustained release of a variety of biologically effective molecules, e.g. antibiotics.[20] For the above reasons, the scaffolds are a highly interesting drug delivery system that would enable constant drug supply over longer time periods at the defect site in the patient.

Conclusions

The experiments showed that the proposed one-step fabrication method is suitable to incorporate sensitive macromolecular drugs into customisable, open-porous resorbable HAp bone substitutes without impairing their activity. The drugs are released by degrees, so that they are effective over a longer time period of at least 9 days.

By incorporating LSZ as an antibacterial agent, an effect on gram-positive bacteria could be observed. Whereas a clear antibacterial effect on *M. luteus* was observed only a bacteriostatic effect was found for *L. innocua*. For the gram-negative bacteria strains which are not affected by LSZ high bacteria proliferation was observed indicating the good bacteria adhesion on HAp surfaces and the necessity for antibacterial agents. Higher LSZ content in the scaffolds led to faster bacteria dieback in the case of *M. luteus* and a 2.5 wt.% LSZ content killed all *M. luteus* bacteria after a very short time (30 min). Scaffolds with a lower LSZ content (0.5 wt.%) also had a sufficient antibacterial effect with a total dieback of *M. luteus* after 24 h.

Sufficient stability for handling could be reached for all scaffold types with HAp scaffolds with 2.5 wt.% LSZ featuring the highest strength of 5.0 MPa along with a porosity of 55%. The highest pore volume and diameters were reached for scaffolds with 0.5 wt.% with 63% total porosity and pore diameters of up to 100 μm.

All these promising results have shown that scaffolds obtained by the one-pot freeze gelation method containing proteins are a potential bone substitute candidate for bone tissue engineering and localised drug delivery of highly bioavailable macromolecular drugs.

Acknowledgements

We thank the German Research Foundation (DFG) for partially funding this project (Project number RE 2735/2-2).

Declaration of Conflicting Interests

The author(s) declared no potential conflicts of interest with respect to the research, authorship, and/or publication of this article.

Funding

The author(s) received no financial support for the research, authorship, and/or publication of this article.

References

1. Ginebra M-P, Canal C, Espanol M, et al. Calcium phosphate cements as drug delivery materials. *Adv Drug Deliv Rev* 2012; 64: 1090–1110.
2. Salgado AJ, Coutinho OP and Reis RL. Bone tissue engineering: State of the art and future trends. *Macromol Biosci* 2004; 4: 743–765.
3. Bose S, Roy M and Bandyopadhyay A. Recent advances in bone tissue engineering scaffolds. *Trends Biotechnol* 2012; 30: 546–554.
4. Simchi A, Tamjid E, Pishbin F, et al. Recent progress in inorganic and composite coatings with bactericidal capability for orthopaedic applications. *Nanomed-Nanotechnol Biol Med* 2011; 7: 22–39.
5. Parent M, Magnaudeix A, Delebassee S, et al. Hydroxyapatite microporous bioceramics as vancomycin reservoir: Antibacterial efficiency and biocompatibility investigation. *J Biomater Appl* 2016; 31: 488–498.
6. Anselmo AC and Mitragotri S. An overview of clinical and commercial impact of drug delivery systems. *J Control Release* 2014; 190: 15–28.
7. Mrsny RJ. Oral drug delivery research in Europe. *J Control Release* 2012; 161: 247–253.
8. Ensign LM, Cone R and Hanes J. Oral drug delivery with polymeric nanoparticles: The gastrointestinal mucus barriers. *Adv Drug Deliv Rev* 2012; 64: 557–570.
9. Krol S. Challenges in drug delivery to the brain: Nature is against us. *J Control Release* 2012; 164: 145–155.
10. Cima MJ, Lee H, Daniel K, et al. Single compartment drug delivery. *J Control Release* 2014; 190: 157–171.
11. Romagnoli C, D'Asta F and Brandi ML. Drug delivery using composite scaffolds in the context of bone tissue engineering. *Clin Cases Mineral Bone Metab* 2013; 10: 155–161.
12. Yang VC, Liang JF and Li YT. Biomedical application of immobilized enzymes. *J Pharm Sci* 2000; 89: 979–990.
13. Kim J, Grate JW and Wang P. Nanostructures for enzyme stabilization. *Chem Eng Sci* 2006; 61: 1017–1026.
14. Blumlein A and McManus JJ. Reversible and non-reversible thermal denaturation of lysozyme with varying

pH at low ionic strength. *Biochim Biophys Acta (BBA) – Proteins Proteom* 2013; 1834: 2064–2070.
15. Cinar S and Czeslik C. Secondary structure and folding stability of proteins adsorbed on silica particles pressure versus temperature denaturation. *Colloids Surf B: Biointerf* 2015; 129: 161–168.
16. Mallamace D, Corsaro C, Vasi C, et al. The protein irreversible denaturation studied by means of the bending vibrational mode. *Phys A: Stat Mech Appl* 2014; 412: 39–44.
17. Park BK, Yi N, Park J, et al. Monitoring protein denaturation using thermal conductivity probe. *Int J Biol Macromol* 2012; 52: 353–357.
18. Scheffler M and Colombo P. *Cellular ceramics*. Pennsylvania, USA: Wiley-VCH Verlag GmbH & Co. KGaA, 2004.
19. Mueller B, Koch D, Lutz R, et al. A novel one-pot process for near-net-shape fabrication of open-porous resorbable hydroxyapatite/protein composites and in vivo assessment. *Mater Sci Eng C* 2014; 42: 137–145.
20. Hess U, Hill S, Treccani L, et al. A mild one-pot process for synthesising hydroxyapatite/biomolecule bone scaffolds for sustained and controlled antibiotic release. *Biomed Mater* 2015; 10: 015013.
21. Hess U, Mikolajczyk G, Treccani L, et al. Multiloaded ceramic beads/matrix scaffolds obtained by combining ionotropic and freeze gelation for sustained and tuneable vancomycin release. *Mater Sci Eng C* 2016; 67: 542–553.
22. Mueller B, Zacharias M and Rezwan K. Bovine serum albumin and lysozyme adsorption on calcium phosphate particles. *Adv Eng Mater (Inside Cover Page)* 2010; 12: B53–B61.
23. Abeyrathne EDNS, Lee HY and Ahn DU. Egg white proteins and their potential use in food processing or as nutraceutical and pharmaceutical agents – A review. *Poult Sci* 2013; 92: 3292–3299.
24. Bauer TW and Smith ST. Bioactive materials in orthopaedic surgery: Overview and regulatory considerations. *Clin Orthopaed Relat Res* 2002; 395: 11–22.
25. Damien CJ and Parsons JR. Bone-graft and bone-graft substitutes – a review of current technology and applications. *J Appl Biomater* 1991; 2: 187–208.
26. Hench LL and Polak JM. Third-generation biomedical materials. *Science* 2002; 295: 1014–1017.
27. Borger A, Supancic P and Danzer R. The ball on three balls test for strength testing of brittle discs: stress distribution in the disc. *J Eur Ceram Soc* 2002; 22: 1425–1436.
28. Ren F, Case ED, Morrison A, et al. Resonant ultrasound spectroscopy measurement of Young's modulus, shear modulus and Poisson's ratio as a function of porosity for alumina and hydroxyapatite. *Philos Mag* 2009; 89: 1163–1182.
29. Bradford MM. A rapid and sensitive method for the quantitation of microgram quantities of protein utilizing the principle of protein-dye binding. *Anal Biochem* 1976; 72: 248–254.
30. Bauer AW, Perry DM and Kirby WMM. Single disc antibiotic sensitivity testing of Staphylococci. *AMA Arch Intern Med* 1959; 104: 208–216.
31. ISO 11137-2:2013. Sterilization of health care products – Radiation – Part 2: Establishing the sterilization dose.
32. Koch D, Andresen L, Schmedders T, et al. Evolution of porosity by freeze casting and sintering of sol-gel derived ceramics. *J Sol-Gel Sci Tech* 2003; 26: 149–152.
33. Hench L. Bioceramics: From concept to clinic. *J Am Ceram Soc* 1991; 74: 1487–1510.
34. Kaplan SJ, Hayes WC, Stone JL, et al. Tensile strength of bovine trabecular bone. *J Biomech* 1985; 18: 723–727.
35. Stone JL, Beaupre GS and Hayes WC. Multiaxial strength characteristics of trabecular bone. *J Biomech* 1983; 16: 743–752.
36. Li WL, Lu K and Walz JY. Freeze casting of porous materials: Review of critical factors in microstructure evolution. *Int Mater Rev* 2012; 57: 37–58.
37. Deville S, Saiz E and Tomsia AP. Freeze casting of hydroxyapatite scaffolds for bone tissue engineering. *Biomaterials* 2006; 27: 5480–5489.
38. McKee CT and Walz JY. Effects of added clay on the properties of freeze-casted composites of silica nanoparticles. *J Am Ceram Soc* 2009; 92: 916–921.
39. Zhang Y, Zuo K and Zeng Y-P. Effects of gelatin addition on the microstructure of freeze-cast porous hydroxyapatite ceramics. *Ceram Int* 2009; 35: 2151–2154.
40. Swain SK and Sarkar D. Preparation of nano-hydroxyapatite gelatin porous scaffold and mechanical properties at cryogenic environment. *Mater Lett* 2013; 92: 252–254.
41. Mishra SK, Shrivastav A and Mishra S. Effect of preservatives for food grade C-PC from *Spirulina platensis*. *Process Biochem* 2008; 43: 339–345.
42. Delwiche J. The impact of perceptual interactions on perceived flavor. *Food Qual Preference* 2004; 15: 137–146.
43. Firouzabadi FB, Noori M, Edalatpanah Y, et al. ZnO nanoparticle suspensions containing citric acid as antimicrobial to control Listeria monocytogenes, *Escherichia coli*, *Staphylococcus aureus* and *Bacillus cereus* in mango juice. *Food Control* 2014; 42: 310–314.
44. Furuta M, Oka M and Hayashi T. Radiation sterilization of enzyme hybrids with biodegradable polymers. *Radiat Phys Chem* 2002; 63: 323–325.
45. Zulli G, Lopes PS, Velasco MVR, et al. Influence of gamma radiation onto polymeric matrix with papain. *Radiat Phys Chem* 2010; 79: 286–288.
46. Ijiri S, Yamamuro T, Nakamura T, et al. Effect of sterilization on bone morphogenetic protein. *J Orthopaed Res* 1994; 12: 628–636.
47. Benkerroum N. Antimicrobial activity of lysozyme with special relevance to milk. *African J Biotechnol* 2008; 7: 4856–4867.
48. Ibrahim HR, Kobayashi K and Kato A. Length of hydrocarbon chain and antimicrobial action to gram-negative bacteria of fatty acylated lysozyme. *J Agric Food Chem* 1993; 41: 1164–1168.
49. Ellison RT and Giehl TJ. Killing of gram-negative bacteria by lactoferrin and lysozyme. *J Clin Invest* 1991; 88: 1080–1091.

50. Guerreiro-Tanomaru JM, de Faria-Junior NB, Duarte MAH, et al. Comparative analysis of *Enterococcus faecalis* biofilm formation on different substrates. *J Endodont* 2013; 39: 346–350.
51. Ichikawa T, Hirota K, Miyake Y, et al. In vitro adherence of *Streptococcus constellatus* to dense hydroxyapatite and titanium. *J Oral Rehab* 1998; 25: 125–127.
52. Li J, Hirota K, Goto T, et al. Biofilm formation of *Candida albicans* on implant overdenture materials and its removal. *J Dentist* 2012; 40: 686–692.